THE JOURNAL OF BIOLOGICAL CHEMISTRY VOL. 282, NO. 50, pp. 36354–36361, December 14, 2007
Printed in the U.S.A.

TBC1D20 Is a Rab1 GTPase-activating Protein That Mediates Hepatitis C Virus Replication*

Received for publication, June 26, 2007, and in revised form, September 26, 2007 Published, JBC Papers in Press, September 27, 2007, DOI 10.1074/jbc.M705221200

Ella H. Sklan[‡1], Ramon L. Serrano[§2], Shirit Einav[‡], Suzanne R. Pfeffer[§], David G. Lambright[¶], and Jeffrey S. Glenn[‡‖3]

From the [‡]Department of Medicine, Division of Gastroenterology and Hepatology, and the [§]Department of Biochemistry, Stanford University School of Medicine, Stanford, California 94305, the [‖]Veterans Affairs Medical Center, Palo Alto, California 94304, and the [¶]Program in Molecular Medicine and the Department of Biochemistry and Molecular Pharmacology, University of Massachusetts Medical School, Worcester, Massachusetts 01605

Like other viruses, productive hepatitis C virus (HCV) infection depends on certain critical host factors. We have recently shown that an interaction between HCV nonstructural protein NS5A and a host protein, TBC1D20, is necessary for efficient HCV replication. TBC1D20 contains a TBC (Tre-2, Bub2, and Cdc16) domain present in most known Rab GTPase-activating proteins (GAPs). The latter are master regulators of vesicular membrane transport, as they control the activity of membrane-associated Rab proteins. To better understand the role of the NS5A-TBC1D20 interaction in the HCV life cycle, we used a biochemical screen to identify the TBC1D20 Rab substrate. TBC1D20 was found to be the first known GAP for Rab1, which is implicated in the regulation of anterograde traffic between the endoplasmic reticulum and the Golgi complex. Mutation of amino acids implicated in Rab GTPase activation by other TBC domain-containing GAPs abrogated the ability of TBC1D20 to activate Rab1 GTPase. Overexpression of TBC1D20 blocked the transport of exogenous vesicular stomatitis virus G protein from the endoplasmic reticulum, validating the involvement of TBC1D20 in this pathway. Rab1 depletion significantly decreased HCV RNA levels, suggesting a role for Rab1 in HCV replication. These results highlight a novel mechanism by which viruses can hijack host cell machinery and suggest an attractive model whereby the NS5A-TBC1D20 interaction may promote viral membrane-associated RNA replication.

Hepatitis C is a major global public health problem. About 170 million people are infected with hepatitis C virus (HCV),[4] and it is the leading cause of liver cancer and liver transplantation in the United States. Current interferon-based therapy is inadequate for most patients (1). HCV is a positive, single-stranded RNA virus containing a 9.6-kb genome encoding a single ~3000-amino acid polyprotein. This polyprotein is proteolytically processed into structural proteins that compose the mature virus and nonstructural proteins that are involved in replicating the viral genome (2). Like other positive strand RNA viruses, HCV is also believed to replicate its RNA in association with intracellular membranes, although the details of replication complex assembly are unknown (3).

HCV NS5A is a phosphoprotein of ~56–58 kDa, depending on its phosphorylation status (4–7). NS5A is anchored to a subset of intracellular membranes via an N-terminal amphipathic α-helix (8, 9) and an unidentified host cell membrane protein (10). Disruption of the amphipathic nature of the helix abolishes NS5A membrane localization and viral replication (9). The NS5A amphipathic α-helix is composed of a hydrophobic face proposed to be embedded in the cytoplasmic leaflet of the endoplasmic reticulum (ER) membrane and a polar charged face that is exposed to the cytosol and thought to mediate specific protein-protein interactions that are essential for the formation of a functional HCV replication complex (11). Because HCV replication is believed to occur on novel membrane structures derived from the ER (2), it would be reasonable to hypothesize that the virus will need to subvert host vesicular membrane transport pathways. That NS5A might be involved in this process is suggested by the reported interaction of NS5A with several proteins that are implicated in intracellular protein trafficking (12–14). Small interfering RNA (siRNA)-mediated depletion of some of these NS5A-interacting partners, such as the SNARE (soluble NSF attachment protein receptors)-like protein human vesicle-associated protein subtype A, was shown to inhibit HCV replication (15).

Another family of proteins known to play critical roles in regulating vesicular membrane trafficking pathways are Rab proteins. Rab GTPases behave as membrane-associated molecular switches (16): they interconvert between an active, GTP-bound form and an inactive, GDP-bound form. Rab GTPases have a very low intrinsic GTPase activity, and they depend on GTPase-activating proteins (GAPs) to activate GTP hydrolysis. Human cells contain as many as 70 Rabs and at least 51 putative Rab GAPs (17). Only a few of these GAPs have been matched to a specific Rab substrate. Rab proteins have been previously implicated in the life cycles of various viruses, including HCV (for example, see Refs. 18–20). These Rabs mediate the endocytosis, trafficking, or sorting of a variety of viral proteins.

* This work was supported in part by a Burroughs Wellcome Fund award and National Institutes of Health Grants RO1-DK064223 (to J. S. G.) and R37-DK37332 (to S. R. P.). The costs of publication of this article were defrayed in part by the payment of page charges. This article must therefore be hereby marked "*advertisement*" in accordance with 18 U.S.C. Section 1734 solely to indicate this fact.
[1] Recipient of an American Liver Foundation postdoctoral research fellow award and an Israel Science Foundation Bikura postdoctoral fellowship.
[2] Supported by a grant from the Susan G. Komen Breast Cancer Foundation.
[3] To whom correspondence should be addressed: Division of Gastroenterology and Hepatology, Stanford University School of Medicine, CCSR Bldg., Rm. 3115, 269 Campus Dr., Palo Alto, CA 94305-5187. Tel.: 650-725-3373; Fax: 650-723-3032; E-mail: jeffrey.glenn@stanford.edu.
[4] The abbreviations used are: HCV, hepatitis C virus; GAP, GTPase-activating protein; siRNA, small interfering RNA; ER, endoplasmic reticulum; GFP, green fluorescent protein; VSV-G, vesicular stomatitis virus G protein.

We have recently discovered the first example of a Rab GAP being exploited by a virus (21). Starting from a yeast two-hybrid screen, HCV NS5A was shown to specifically interact with the host cell protein TBC1D20 (21). The latter contains a TBC domain present in most known Rab GAPs (22). Depletion of TBC1D20 severely impairs HCV replication and prevents new infection, with minimal effects on cell viability (21). These exciting results raised several key questions regarding the physiological role of TBC1D20 in host cells and in viral replication. We present here experiments that identify TBC1D20 as the Rab GAP for Rab1 and suggest an attractive mechanism used by HCV to subvert host cell machinery for the promotion of viral replication.

EXPERIMENTAL PROCEDURES

Cell Culture and Transfections—Monolayers of the human hepatoma cell line Huh7.5 (23) were grown routinely as described (24). Cells were passaged twice weekly after treatment with 0.05% trypsin, 0.02% EDTA and seeded at a dilution of 1:3. BSC-1 cells were grown in α-minimum Eagle's medium supplemented with 1% L-glutamine (Invitrogen), 1% penicillin, 1% streptomycin, 7.5% fetal bovine serum. BSC-1 cells were passaged twice weekly after treatment with 0.25% trypsin, 0.02% EDTA and seeding at a dilution of 1:3. HeLa cells were grown in complete Dulbecco's modified Eagle's medium supplemented with 1% L-glutamine, 1% penicillin, 1% streptomycin, and 10% fetal bovine serum. Cells were passaged twice weekly and seeded at a dilution of 1:3. Huh7 and Huh7.5 cells were transfected using Lipofectamine 2000 (Invitrogen) according to the manufacturer. HeLa and BSC-1 cells were transfected using FuGENE 6 (Roche Applied Science).

Plasmids—Standard recombinant DNA technology was used to construct and purify all plasmids. All regions that were amplified by PCR were analyzed by automated DNA sequencing. Plasmid DNA was prepared from large-scale bacterial cultures and purified by a Maxiprep kit (Marligen Biosciences). Restriction enzymes were purchased from New England Biolabs.

The plasmid pE green fluorescent protein (GFP)-TBC1D20 was made by cloning full-length TBC1D20 (GenBank™ accession number NM_144628) obtained from the yeast two-hybrid positive clone into pEGFP-C1 (Clontech). pEGFP-TBC1D20 R105A was made by introduction of the R105A mutation using the QuikChange site-directed mutagenesis kit (Stratagene). pMyc-TBC1D20 and pMyc-TBC1D20 R105A were created similarly in pCMV-Myc (Clontech). The plasmid expressing the vesicular stomatitis virus G protein (VSV-G) fused to yellow fluorescent protein was a generous gift from Dr. Benjamin Aroeti. The Rab constructs were described elsewhere (25). pDEST-17 for bacterial expression of TBC1D20 with a His_6 N-terminal tag was prepared from a Gateway system (Invitrogen) entry clone for TBC1D20 obtained from the Human ORFeome Collection (Open Biosystems catalog no. OHS1771). The R66A and R105A mutations were inserted in to pDEST-17-TBC1D20 using the QuikChange site-directed mutagenesis kit. To express TBC1D20 amino acids 1–362, the TBC1D20 fragment was amplified by PCR and cloned into pET14b in-frame with the N-terminal His tag.

Immunofluorescence—BSC-1 or HeLa cells were grown on coverslips. The cells were fixed 18 h post-transfection using 4% formaldehyde. Following fixation, the cells were permeabilized with saponin and stained with an anti-calnexin antibody (1:200, StressGen), anti-GM130 monoclonal antibody (1:1000, Transduction Labs), or anti-Myc primary antibody (1:1000, Santa Cruz Biotechnology), followed by secondary goat anti-mouse antibodies conjugated to Alexa 594. Coverslips were mounted with polyvinyl alcohol (Mowiol) mounting medium.

Fluorescence images were captured with a Nikon E600 fluorescence microscope equipped with a SPOT digital camera and Openlab image acquisition software (Improvision). Confocal images were taken using a Bio-Rad confocal microscope.

Bacterial Expression and Purification—Purification of Rab proteins was described elsewhere (25). For the purification of TBC1D20 and TBC1D20 R66A,R105A, pDEST-17 containing each of these proteins was transformed into BL21-CodonPlus(DE3)-RIPL cells (Stratagene). pET14b-TBC1D20 amino acids 1–362 were transformed into Rosetta cells (Invitrogen). Overnight cultures of *Escherichia coli* were diluted 1:100 in 500 ml of fresh medium and grown at 37 °C to an absorbance of 1. Isopropyl β-D-thiogalactopyranoside (Invitrogen) was then added to a final concentration of 1 mM. After 3 h of growth, cells were pelleted and resuspended in 25 ml of lysis buffer (50 mM Tris (pH 8), 400 mM NaCl, and 0.1% Fos-Choline-13 (Anatrace Inc.), and Complete mini protease inhibitor tablets (Roche Applied Science)). After 15 min of incubation on ice, cells were lysed by two cycles in a French press at a pressure of 10,000 p.s.i. for 1 min, followed by centrifugation at 27,000 $\times$ *g* for 30 min at 4 °C. The supernatant was then passed through a 0.45-μm filter and loaded on a 1-ml HisTrap nickel-nitrilotriacetic acid column (GE Healthcare) in the presence of 20 mM imidazole (Sigma). Following two washes with lysis buffer, TBC1D20 was eluted in 2 ml of elution buffer (50 mM Tris (pH 8), 400 mM NaCl, 0.1% Fos-Choline-13, and 400 mM imidazole). The pooled eluates were loaded onto a Superdex 200 column (HiLoad Superdex 200 prep grade, 26/60; GE Healthcare) pre-equilibrated with Superdex 200 buffer (20 mM HEPES (pH 7.4), 200 mM NaCl, and 1 mM $MgCl_2$). Fractions containing TBC1D20 monomer were pooled and stored at −80 °C. Expression and purification were monitored by SDS-PAGE, followed by Coomassie staining or Western blot analysis with an anti-His_6 antibody (1:5000, Pharmingen). There were no differences in yield or purity between the mutant proteins and wild-type TBC1D20.

GAP Assays—GAP assays were previously described (25). Briefly, Rab GTPases were loaded with GTP by incubating 2–3 mg of protein with a 25-fold molar excess of GTP at 25 °C for 1 h in 20 mM HEPES (pH 7.5), 150 mM NaCl, 5 mM EDTA, and 1 mM dithiothreitol. Free nucleotide was then removed using D-Salt columns (Pierce) pre-equilibrated with 20 mM HEPES (pH 7.5) and 150 mM NaCl. The kinetics of intrinsic and GAP-accelerated GTP hydrolysis were measured by a continuous enzyme-coupled optical assay for the release of inorganic phosphate, with the use of reagents from the EnzChek phosphate assay kit (Invitrogen). GTP-loaded Rab GTPases were mixed with solutions containing the assay reagents and GAPs and dispensed into 96-well half-area microplates (Corning) using a Precision

2000 pipetting system (Bio-Tek). The final solutions contained 20 mM HEPES (pH 7.5), 150 mM NaCl, 0.15 mM 2-amino-6-mercapto-7-methylpurine ribonucleoside, 0.75 unit/ml purine nucleoside phosphorylase, 10 mM $MgCl_2$, 20 mM GTP-loaded Rab GTPases, and various concentrations of GAPs. Absorbance at 360 nm was monitored with a Safire microplate spectrometer (Tecan).

Data were analyzed by fitting them simultaneously to the pseudo-first-order Michaelis-Menten model function (see Ref. 25). The catalytic efficiency (k_{cat}/K_m) and intrinsic rate constant for GTP hydrolysis (k_{intr}) were treated as global parameters.

Carbonate Extraction of Membranes—A confluent 10-cm^2 dish of Huh7 cells was transfected with GFP-TBC1D20. The cells were trypsinized 24 h post-transfection, washed twice with phosphate-buffered saline supplemented with protease inhibitors, and homogenized with 50 passes through a 25-gauge needle. Breakage of the cells was confirmed using trypan blue exclusion. The supernatants were cleared at 500 × *g* and split into two equal volumes. Membranes were then pelleted by a 30-min centrifugation at 100,000 × *g* in a Beckman TL-100 ultracentrifuge. The supernatant was saved as the cytosolic fraction, and the membranes were resuspended in 10 volumes of 0.3 M sucrose in 10 mM Tris (pH 7). An additional 10 volumes containing 10 mM Tris (pH 7) or 0.2 M sodium carbonate (pH 11) (27) were added to the control and treated tube, respectively, followed by a 30-min incubation on ice. The homogenates were then spun at 100,000 × *g* for 1 h at 4 °C. Membranes were resuspended directly in sample buffer, and the supernatants were precipitated using methanol/chloroform precipitation and resuspended in sample buffer. Equivalent volumes of each sample were loaded on the gel and analyzed by immunoblot with anti-GFP antibodies (1:1000, Molecular Probes).

VSV-G Trafficking Assays—HeLa cells were grown on coverslips and cotransfected with the VSV-G-yellow fluorescent protein (ts 045) expression plasmid and pCMV-Myc-TBC1D20 or the R105A mutant. The transfected cells were transferred to 40 °C 2 h post-transfection, and they were incubated for 16 h. The cells were then incubated at 32 °C for the appropriate chase period, followed by formaldehyde fixation and immunostaining.

siRNAs—All siRNAs were purchased from Dharmacon as duplexes. si*CONTROL* non-targeting siRNA #1 (Dharmacon) was used as a negative control. Rab1B siRNAs were as follows: Duplex 9, 5′-UGCAGGAGAUUGACCGCUAUU-3′ (sense) and 5′-UAGCGGUCAAUCUCCUGCAUU-3′ (antisense); Duplex 10, 5′-CCAGCGCGAACGUCAAUAAUU-3′ (sense) and 5′-UUAUUGACGUUCUCGCUGGUU-3′ (antisense); Duplex 11, 5′-CGGUGGGAUCUGAGUAUAUUU-3′ (sense) and 5′-AUAUACUCAGAUCCCACCGUU-3′ (antisense); and Duplex 12, 5′-GAAUAUGACUACCUGUUUAUU-3′ (sense) and 5′-UAAACAGGUAGUCAUAUUCUU-3′ (antisense). siRNA transfections were done using 100 nM siRNA/well in a 6-well plate.

Real-time PCR—For real-time PCR experiments, Huh7.5 cells were transfected with *siCONTROL* or Rab1B siRNAs. The cells were trypsinized 8 h after transfection, and 1×10^5 cells were plated in a 12-well plate. The cells were allowed to adhere overnight and were infected with cell culture-grown HCV titered at 1.4×10^4 TCID50/ml, as described (28, 29). 2 h after infection, cells were washed twice with the medium. After 72 h, RNA was extracted in triplicates using 0.5 ml of TRIzol reagent (Invitrogen) and then subjected to reverse transcription using random hexamers and SuperScript II reverse transcriptase (Invitrogen). Real-time PCR was performed on the resulting cDNA to quantify the amount of Rab1B, HCV, and actin RNAs (in separate reactions) in each sample, as compared with an *in vitro* transcribed HCV RNA standard and human actin standard (Applied Biosystems, Foster City, CA), respectively. HCV was quantified using primers AGAGCCATAGTGGTCT and CCAAATCTCCAGGCATTGAGC and probe 6-carboxyfluorescein-CACCGGAATTGCCAGGACGACCGG-6-carboxytetramethylrhodamine. Actin was quantified using β-actin control reagents (Applied Biosystems) according to the manufacturer's instructions. Rab1B was quantified using the TaqMan® gene expression assays probe and primer set for Rab1B (Assay ID Hs00823717_g1).

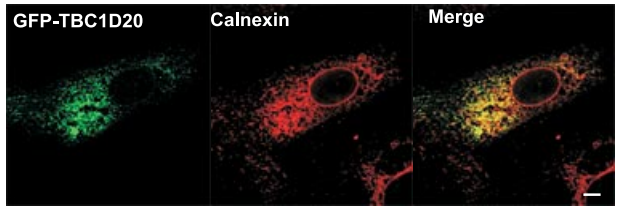

FIGURE 1. **TBC1D20 is localized to the ER.** GFP-TBC1D20 was transfected into BSC-1 cells, and 24 h after transfection cells were fixed and stained with anti-calnexin antibody. Co-localization was confirmed using confocal microscopy. *Scale bar* = 5 μm.

RESULTS

TBC1D20 Is a Rab1 GAP—Human cells are predicted to have as many as 70 Rabs. To narrow down the number of potential substrates for the TBC1D20 GAP, we characterized the subcellular distribution of TBC1D20. When BSC-1 cells were transfected with a plasmid expressing TBC1D20 with an N-terminal GFP tag, a reticular pattern typical of ER localization was observed (Fig. 1). Confocal microscopy showed that in all the TBC1D20-expressing cells most of the TBC1D20 signal co-localized with the ER marker calnexin, confirming its ER localization. Based on this apparent ER localization, we predicted that the Rabs regulated by TBC1D20 are likely to be those associated with the ER. Because an apparent interaction between HCV NS4B and Rab5 was recently reported (18) and because some Rabs are known to be activated by more than one GAP (30, 31), we performed a broader screen including 27 mammalian Rabs. The GAP Gyp1 (whose Rab substrates are known) was tested against Rab1, -2, -3, and -33 as a control for the specificity and activity of the Rabs tested (25). Among the Rabs tested, TBC1D20 had a high selectivity for activating the Rab1 GTPase (Fig. 2). The activity of TBC1D20 was further investigated by simultaneous fitting of the data to a pseudo-first-order Michaelis-Menten model function. Activation of Rab1 GTP hydrolysis by TBC1D20 has an apparent catalytic efficiency (k_{cat}/K_m) of 360 M^{-1} s^{-1} (Fig. 3*A*). A recent crystallographic study revealed that Rab GAPs activate their Rab GTPase substrates via a so-called "dual finger" mechanism involving two critical catalytic

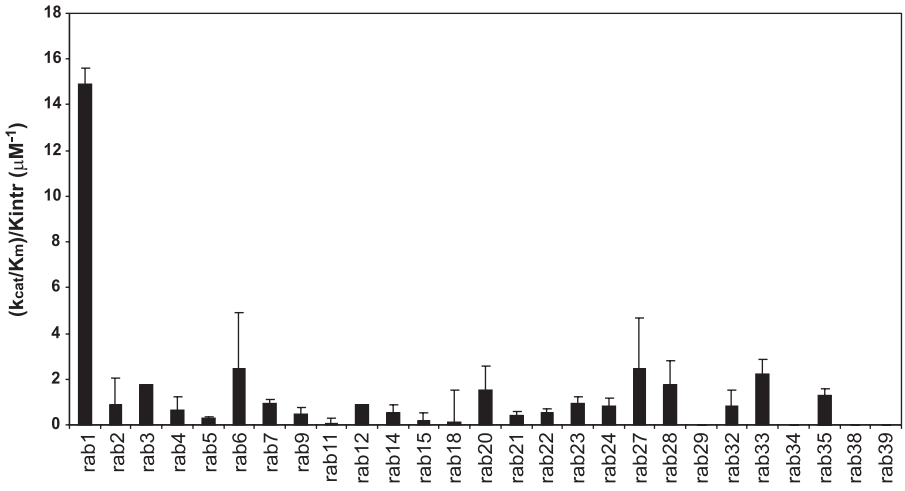

FIGURE 2. **TBC1D20 is a Rab1 GAP.** Purified TBC1D20 was reacted with 27 mammalian Rab GTPases. Catalytic efficiency (k_{cat}/K_m) relative to the intrinsic rate constant for GTP hydrolysis was determined. Values represent the mean from duplicate wells. Note that only Rab1 displays significant activation by TBC1D20.

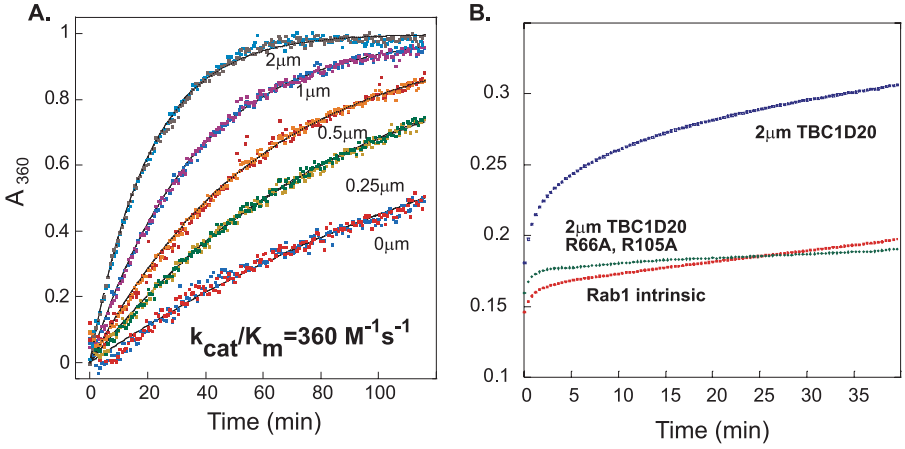

FIGURE 3. **GTP hydrolysis by Rab1 is enhanced by TBC1D20.** *A*, GTP hydrolysis for Rab1 in the presence of increasing concentrations of TBC1D20. *Solid lines* represent a simultaneously fitted pseudo-first-order Michaelis-Menten model function from which catalytic efficiency values were extracted. *B*, kinetics of GTP hydrolysis for Rab1 in the presence of wild-type or TBC domain mutant forms of TBC1D20.

residues supplied in *trans* by the TBC domain (25). We therefore introduced two point mutations into the TBC domain of TBC1D20 to disrupt one of the above "fingers" and determined the ability of the resulting mutant TBC1D20 (R66A,R105A) to activate Rab1 GTPase activity. As shown in Fig. 3*B*, the GTPase-activating activity of TBC1D20 on Rab1 was abolished when these conserved arginine residues were mutated to alanine.

TBC1D20 Is a Transmembrane Protein—Hydropathy analysis of the primary sequence of TBC1D20 using the SOSUI prediction system (32) revealed a C-terminal hydrophobic domain of 26 residues (Fig. 4, *A* and *B*). We hypothesized that the latter represents a transmembrane domain within TBC1D20. Experimental support for this hypothesis came during its purification. The amount of protein purified was extremely low without the presence of a detergent. Alkaline stripping was used to further confirm that TBC1D20 associates with membranes in a manner characteristic of integral membrane proteins. For this, Huh7 cells expressing GFP-TBC1D20 were homogenized, and lysates were separated into cytosolic and membrane fractions by centrifugation. Membranes were then washed with either sodium carbonate or buffer and incubated on ice for 30 min. Membranes were pelleted by centrifugation and analyzed by SDS-PAGE and immunobloting. The GFP-tagged TBC1D20 was found exclusively in the membrane fraction and was resistant to alkaline extraction (Fig. 4*C*), consistent with the notion that TBC1D20 is an integral membrane protein.

The presence of a transmembrane domain might cause aggregation of the purified TBC1D20 *in vitro*, affecting the efficiency of its GAP activity. Indeed, a TBC1D20 truncated form (amino acids 1–362) lacking the transmembrane domain was ~10-fold more efficient (k_{cat}/K_m = 2700 M^{-1} s^{-1}) than the full-length protein (Fig. 4*D*).

Overexpression of TBC1D20 Induces Golgi Disruption—Rab1 is essential for the biogenesis of the Golgi complex (33). Dominant negative forms of Rab1 and Rab1 depletion were shown to alter the structural integrity of the Golgi (33–35), whereas overexpression of the wild-type Rab1 or its constitutively active form did not. If TBC1D20 is indeed a Rab1 GAP *in vivo*, manipulation of TBC1D20 levels might influence Golgi morphology. To test this possibility, HeLa cells were transfected with a plasmid expressing TBC1D20 and its catalytically inactive mutant TBC1D20 R105A, both fused to GFP. In 90% of cells overexpressing the catalytically active form of TBC1D20, the Golgi complex was disrupted, as determined by the redistribution of GM130 to scattered punctate cytoplasmic structures (Fig. 5). Similar results were obtained with other Golgi markers, including p115 (36) (data not shown) and β-coatomer (37). No apparent changes in Golgi morphology were detected when the catalytically inactive mutant TBC1D20 R105A was overexpressed (Fig. 5) or upon TBC1D20 depletion (data not shown). While the manuscript was under review, a similar effect of overexpression of TBC1D20 on Golgi integrity was reported (38).

Overexpression of TBC1D20 Affects ER-to-Golgi Transport—Given that Rab1 is essential for ER-to-Golgi vesicle trafficking (33, 35, 39, 40), manipulation of Rab1 GAP levels would be expected to alter this pathway. Thus, we examined the effect of overexpression of TBC1D20 on the transport of the temperature-sensitive variant (ts 045) of VSV-G. VSV-G (ts 045) protein reversibly misfolds and is retained in the ER at 40 °C, but upon shift to 32 °C it correctly folds and is exported from the ER. As shown in Fig. 6*A*, transfection of cells with Myc-TBC1D20 prevented the exit of VSV-G from the ER in ~80% of

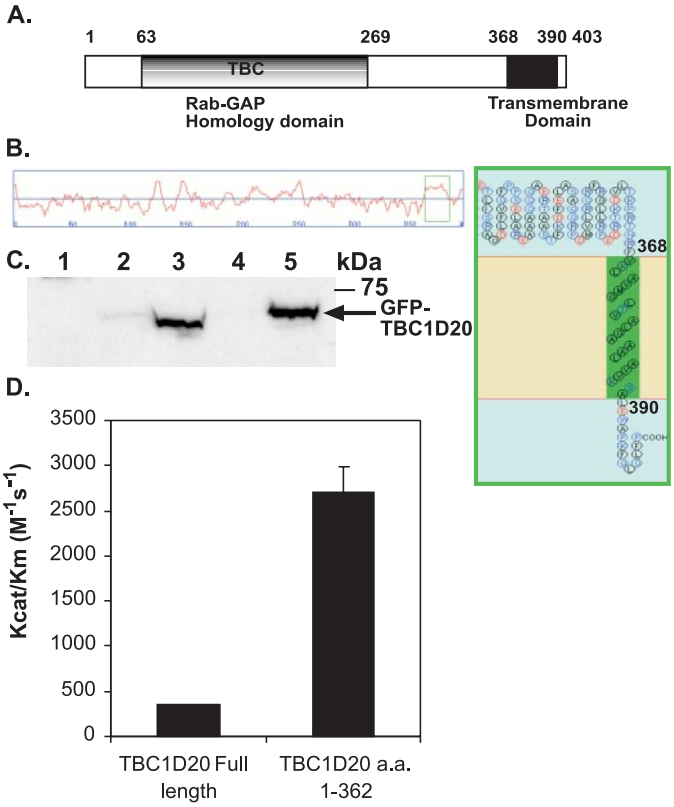

FIGURE 4. **TBC1D20 is a transmembrane protein.** *A*: schematic diagram of TBC1D20. The predicted transmembrane domain is shown in *black* at the C terminus (at the *right*); the TBC domain is indicated. *B*: *left*, graphical output of the SOSUI analysis, with the 403 amino acid residues of TBC1D20 indicated along the *x* axis. The *red line* describes the hydropathy profile of each segment. *Right*, a schematic diagram of the predicted transmembrane domain. *C*: TBC1D20 membrane association is resistant to alkaline stripping. GFP-TBC1D20 membranes were washed with 0.1 M sodium carbonate or buffer and pelleted by centrifugation. Equal amounts of cytosol (*lane 1*) and released proteins and membranes, treated with buffer (*lanes 2* and *3*) or alkaline carbonate (*lanes 4* and *5*), respectively, were loaded and analyzed by SDS-PAGE and immunoblotting with anti-GFP antibodies. *D*: catalytic efficiencies (k_{cat}/K_m) of full-length (wild-type) TBC1D20 or a truncated form (amino acids (*a.a.*) 1–362) lacking the transmembrane domain.

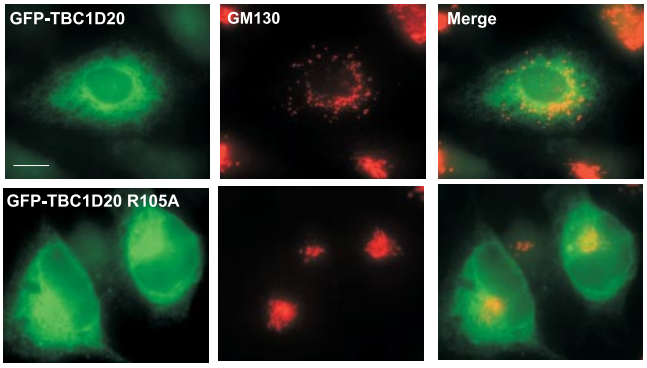

FIGURE 5. **Overexpression of catalytically active TBC1D20 causes disruption of the Golgi complex.** HeLa cells were cotransfected with TBC1D20 or its catalytically inactive mutant R105A, both fused to GFP. The cells were fixed after 20 h and stained with anti-GM130 primary and Alexa 594-conjugated secondary antibodies. *Scale bar* = 10 μm.

the cotransfected cells, even after 60 min of incubation at the permissive temperature. In contrast, upon overexpression of the catalytically inactive mutant Myc-TBC1D20 R105A, VSV-G was found in the Golgi as early as 20 min into the chase

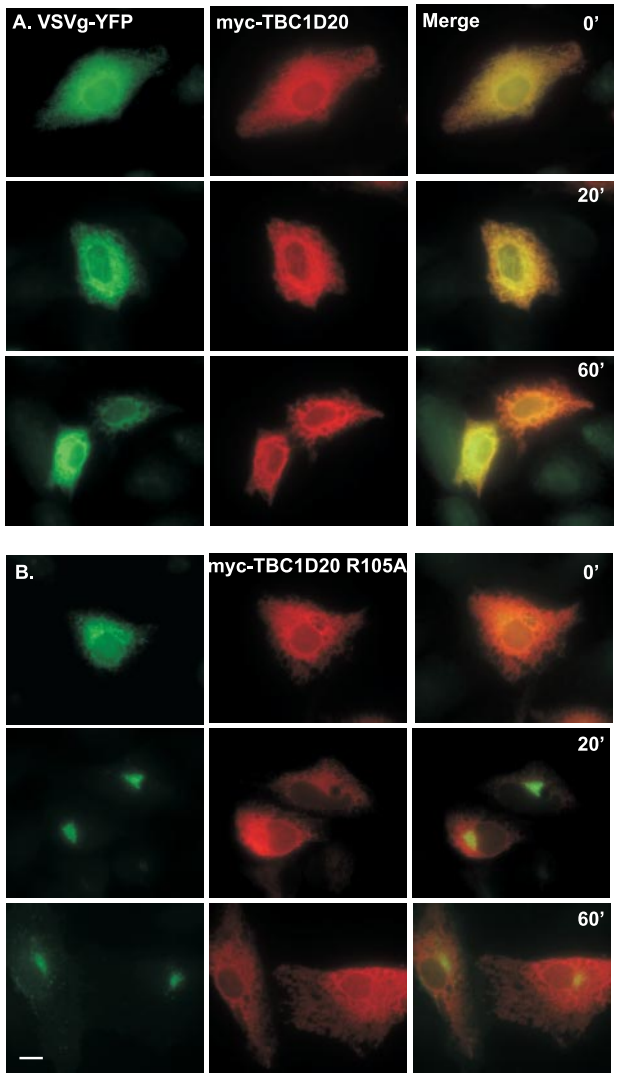

FIGURE 6. **TBC1D20 overexpression blocks ER-to-Golgi transport of VSV-G.** HeLa cells were cotransfected with a yellow fluorescent protein-tagged, temperature-sensitive VSV-G and Myc-tagged wild-type (*A*), or the catalytically inactive mutant (*B*) of TBC1D20. Following a 16-h incubation at the nonpermissive temperature, the cells were shifted to 32 °C for the indicated time periods, fixed, and immunostained using anti-Myc antibodies. *Scale bar* = 10 μm.

period (Fig. 6*B*). These results demonstrate that TBC1D20 regulates Rab1-mediated ER-to-Golgi transport in cultured cells in a manner consistent with its *in vitro* biochemical GAP activity.

Depletion of Rab1 Inhibits Accumulation of HCV RNA—We have recently shown that TBC1D20 depletion inhibits HCV replication and prevents the accumulation of viral RNA (21). If the role of TBC1D20 in the viral life cycle is mediated via its Rab1 substrate, Rab1 depletion should also impair viral RNA accumulation. To test this prediction, we first treated Huh7.5 cells with a control or one of four different Rab1B siRNA duplexes, followed by infection with HCV (genotype 2a, produced *in vitro*, as described (28)). The Rab1B isoform was selected, as it is reported to be the most abundant form of Rab1 in the liver (41).

The efficiency of these siRNAs in decreasing endogenous Rab1B RNA levels was first determined (Fig. 7*A*). Endogenous Rab1B RNA levels were significantly reduced (80%) 96 h after

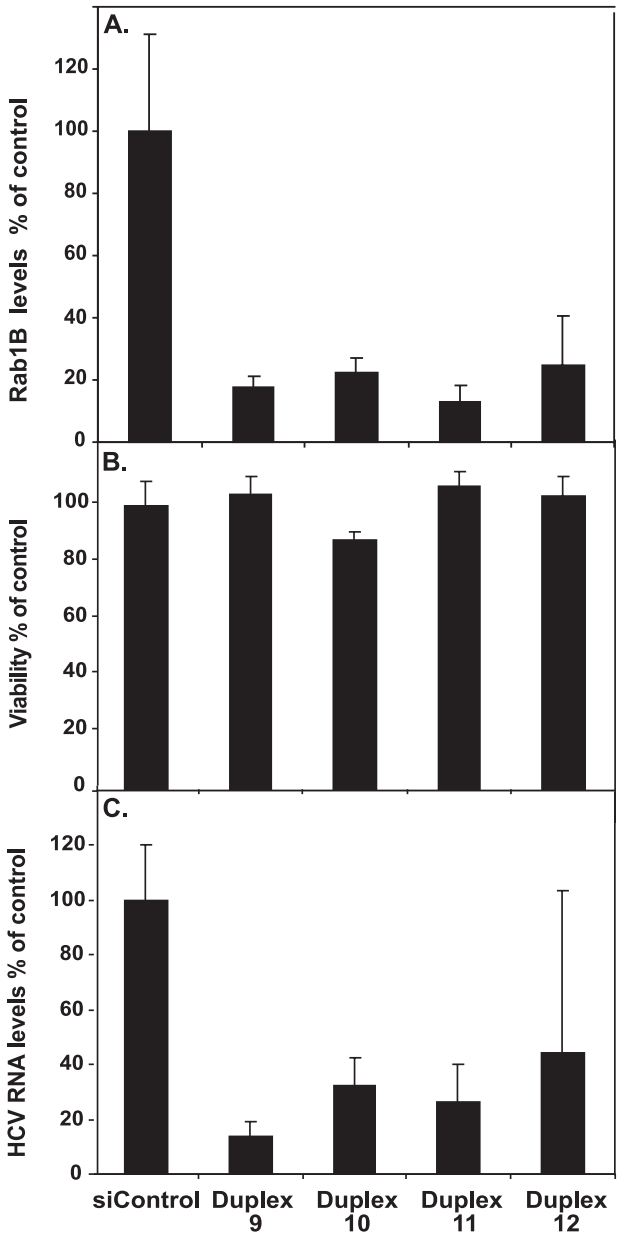

FIGURE 7. **Rab1 depletion reduces HCV RNA levels.** Huh7.5 cells were transfected with one of four different Rab1B siRNA duplexes (Duplexes 9–12), or a control nontargeting siRNA (si*CONTROL*). After transfections (8 h), cells were trypsinized and plated in 12-well plates. The cells were allowed to adhere overnight and then infected with tissue culture grown HCV. Total cellular RNA was harvested after 72 h, followed by real-time PCR assay. *A*, endogenous Rab1B levels were detected 96 h after transfection to assess the knockdown efficiency of the respective siRNAs. *B*, Alamar Blue assays for cell viability were performed 96 h following transfection of anti-Rab1b siRNAs. *C*, following infection (72 h), HCV RNA levels were detected by quantitative real-time PCR. Values (mean ± S.D.) from three independent wells are shown. Results were normalized to actin RNA levels.

siRNA transfection. The same samples were then assayed for HCV RNA (Fig. 7*C*). Viral RNA levels in Rab1B siRNA-treated cells were reduced by 60–85% 72 h after infection compared with control samples. The extent of HCV inhibition as a result of Rab1B depletion was equal to or greater than that observed with inhibition of other host targets reported to play a role in HCV replication (15, 18). This effect was not seen in the cells transfected with the control siRNA, consistent with a role for TBC1D20 and Rab1 in HCV RNA production. Rab1 siRNA treatments had no apparent effect on cell viability 96 h post-transfection (Fig. 7*B*).

DISCUSSION

Like other positive strand RNA viruses, HCV is believed to replicate in association with intracellular membranes. The cellular factors contributing to the organization of this replication complex are largely unknown, although they are likely to include key proteins involved in host vesicular transport pathways. We have recently shown an interaction between NS5A and a host protein, TBC1D20, that mediates viral replication (21). TBC1D20 contains a Rab GAP domain implicated in activating Rab GTPases (42). Here we showed that TBC1D20 was a GAP for Rab1, the Rab involved in the regulation of ER-to-Golgi transport (33, 35, 39, 40). Overexpression of TBC1D20 caused disruption of Golgi morphology and blocked ER-to-Golgi transport of VSV-G, further validating the involvement of TBC1D20 in this pathway. Depletion of Rab1 significantly decreased HCV RNA levels, suggesting a critical role for Rab1 in HCV replication.

We used a biochemical screen to identify the Rab substrate for TBC1D20 (Fig. 2). Of all the Rabs tested, our screen showed that Rab1 is the preferred substrate for TBC1D20. We further examined the biochemical properties of this interaction by simultaneously fitting the data to a pseudo-first-order Michaelis-Menten model. The apparent catalytic efficiency (k_{cat}/K_m) of Rab1 activation by TBC1D20 was 360 M^{-1} s^{-1} (Fig. 3*A*).

Of 50 GAPs predicted to exist in human cells, only a small number are currently matched to their Rab substrates. Two Rab GAPs were initially described for Rab5, the most studied Rab GTPase: RN-Tre (43) and prostate cancer gene 17 (44). Rab5 GAP was described using a yeast two-hybrid library with GTP-locked human Rabs (45). In this screen, RN-Tre also showed an interaction with Rab43 and Rab30. Among other human GAPs described are AS160 (Akt substrate of 160 kDa or TBC1D446), which showed GAP activity for Rab2A, -8A, -10, and -14 (46); GAPCenA, which was shown to activate Rab6 (47), although full-length GAPCenA showed increased activity toward Rab4 (48); EVI5, a centrosomal protein in interphase cells that showed GAP activity toward RAB11 (49); EPI64, a specific Rab27A GAP (50); TBC1D15, which shows a preference for Rab7 (51); and a GAP for Rab3A that was purified from rat brain (52). The range of the published k_{cat}/K_m values for these enzymes is 3333.3–41,666 M^{-1} s^{-1}. Our measured TBC1D20 GAP activity is ~10-fold less efficient. But this *in vitro* difference was explained by the presence of a predicted transmembrane domain at the C terminus because a purified truncated form of TBC1D20 (1–362) had an 8-fold higher k_{cat}/K_m value (2700 M^{-1} s^{-1}) (Fig. 4*D*). TBC1D20 is the first described Rab GAP containing a transmembrane domain.

Much of our knowledge to date concerning Rab GTPases and their GAPs comes from yeast studies. The closest yeast GAP to TBC1D20, based on homology, is Gyp8 (26% identity (53)). Gratifyingly, Gyp8 shows GAP activity toward Ypt1p, the yeast Rab1 homolog (75 and 66% identity to Rab1A and Rab1B, respectively).

An additional GAP for Ypt1p, Gyp5, has also been identified (53). De Antoni *et al.* (52) preformed chromosomal deletions of

either *GYP8* or *GYP5* genes in yeast, and the effect was phenotypically neutral, suggesting overlapping substrate specificity. The lack of effect on cell viability observed upon siRNA depletion of TBC1D20 suggests a similar type of functional duplication (21). Further evidence for possible redundancy is that like Gyp8, Gyp1 is also a GAP for Ypt1 in yeast (54).

The finding that TBC1D20 activates an ER Rab matches well the apparent ER localization of TBC1D20 (Fig. 1) and the postulate that the membrane-associated HCV replication complex is assembled using ER-derived membranes containing the viral proteins. The effect of TBC1D20 overexpression on ER-to-Golgi transport (Fig. 6, *A* and *B*) provides evidence of functional involvement of TBC1D20 in this pathway, further validating our assignment of Rab1 as a substrate for the TBC1D20 GAP activity.

Moreover, the fact that overexpression of catalytically active TBC1D20 disrupts the integrity of the Golgi complex (phenocopying overexpression of a dominant negative Rab1 (33, 35) or Rab1 depletion (34)) further strengthens the role of TBC1D20 as an *in vivo* Rab1 GAP (45). Rab1 depletion significantly decreased HCV RNA levels, strongly implicating a role for Rab1 in HCV replication (Fig. 7).

Rab1 has previously been shown to be recruited to a replication complex of an intracellular pathogen (55, 56). There, a bacterial protein mimics a Rab guanine nucleotide exchange factor, which activates Rab1 and stabilizes it on an organelle that supports bacterial replication, thereby subverting membrane transport from the endoplasmic reticulum. We believe that a similar mechanism might apply for the NS5A-TBC1D20 interaction. Here, GAP interaction might involve local inactivation of Rab1, permitting the formation of the viral replication complex without blocking all ER export. This model is supported by overexpression of NS5A being previously shown to cause an ~20% decrease in the rate of acquisition of Golgi-specific modifications of the VSV-G ts 045/GFP protein (26).

Taken together, these results suggest an attractive model employed by HCV to redirect host cell membrane trafficking machinery to the enhancement of viral replication. We propose that the NS5A-TBC1D20 interaction locally inactivates Rab1 GTPase at sites of nascent viral protein synthesis to promote redirection from a Golgi-bound pathway to the virus-induced membrane structures, supporting HCV RNA replication.

Acknowledgments—We thank Charles Rice for the infectious HCV clone, Anna Delprato for providing critical reagents, and Ian Ganley for fruitful discussions.

REFERENCES

1. Williams, R. (2006) *Hepatology* **44,** 521–526
2. Moradpour, D., Penin, F., and Rice, C. M. (2007) *Nat. Rev. Microbiol.* **5,** 453–463
3. Moradpour, D., Gosert, R., Egger, D., Penin, F., Blum, H. E., and Bienz, K. (2003) *Antiviral Res.* **60,** 103–109
4. Tanji, Y., Kaneko, T., Satoh, S., and Shimotohno, K. (1995) *J. Virol.* **69,** 3980–3986
5. Evans, M. J., Rice, C. M., and Goff, S. P. (2004) *Proc. Natl. Acad. Sci. U. S. A.* **101,** 13038–13043
6. Neddermann, P., Clementi, A., and De Francesco, R. (1999) *J. Virol.* **73,** 9984–9991
7. Appel, N., Pietschmann, T., and Bartenschlager, R. (2005) *J. Virol.* **79,** 3187–3194
8. Brass, V., Bieck, E., Montserret, R., Wolk, B., Hellings, J. A., Blum, H. E., Penin, F., and Moradpour, D. (2002) *J. Biol. Chem.* **277,** 8130–8139
9. Elazar, M., Cheong, K. H., Liu, P., Greenberg, H. B., Rice, C. M., and Glenn, J. S. (2003) *J. Virol.* **77,** 6055–6061
10. Cho, N.-J., Cheong, K. H., Lee, C., Frank, C. W., and Glenn, J. S. (2007) *J. Virol.* **81,** 6682–6689
11. Penin, F., Brass, V., Appel, N., Ramboarina, S., Montserret, R., Ficheux, D., Blum, H. E., Bartenschlager, R., and Moradpour, D. (2004) *J. Biol. Chem.* **279,** 40835–40843
12. Shi, S. T., Polyak, S. J., Tu, H., Taylor, D. R., Gretch, D. R., and Lai, M. M. (2002) *Virology* **292,** 198–210
13. Zech, B., Kurtenbach, A., Krieger, N., Strand, D., Blencke, S., Morbitzer, M., Salassidis, K., Cotten, M., Wissing, J., Obert, S., Bartenschlager, R., Herget, T., and Daub, H. (2003) *J Gen. Virol.* **84,** 555–560
14. Tu, H., Gao, L., Shi, S. T., Taylor, D. R., Yang, T., Mircheff, A. K., Wen, Y., Gorbalenya, A. E., Hwang, S. B., and Lai, M. M. (1999) *Virology* **263,** 30–41
15. Xue, Q., Ding, H., Liu, M., Zhao, P., Gao, J., Ren, H., Liu, Y., and Qi, Z. T. (2007) *Arch. Virol.* **152,** 955–962
16. Zerial, M., and McBride, H. (2001) *Nat. Rev. Mol. Cell Biol.* **2,** 107–117
17. Pfeffer, S. (2005) *Nat. Cell Biol.* **7,** 856–857
18. Stone, M., Jia, S., Do Heo, W., Meyer, T., and Konan, K. V. (2007) *J. Virol.* **81,** 4551–4563
19. Krishnan, M. N., Sukumaran, B., Pal, U., Agaisse, H., Murray, J. L., Hodge, T. W., and Fikrig, E. (2007) *J. Virol.* **81,** 4881–4885
20. Vonderheit, A., and Helenius, A. (2005) *PLoS Biol.* **3,** 1225–1238
21. Sklan, E. H., Staschke, K., Oakes, T. M., Elazar, M., Winters, M., Aroeti, B., Danieli, T., and Glenn, J. S. (2007) *J. Virol.* **81,** 11096–11105
22. Bernards, A., and Settleman, J. (2004) *Trends Cell Biol.* **14,** 377–385
23. Blight, K. J., McKeating, J. A., and Rice, C. M. (2002) *J. Virol.* **76,** 13001–13014
24. Einav, S., Elazar, M., Danieli, T., and Glenn, J. S. (2004) *J. Virol.* **78,** 11288–11295
25. Pan, X., Eathiraj, S., Munson, M., and Lambright, D. G. (2006) *Nature* **442,** 303–306
26. Konan, K. V., Giddings, T. H., Jr., Ikeda, M., Li, K., Lemon, S. M., and Kirkegaard, K. (2003) *J. Virol.* **77,** 7843–7855
27. Fujiki, Y., Hubbard, A. L., Fowler, S., and Lazarow, P. B. (1982) *J. Cell Biol.* **93,** 97–102
28. Lindenbach, B. D., Evans, M. J., Syder, A. J., Wolk, B., Tellinghuisen, T. L., Liu, C. C., Maruyama, T., Hynes, R. O., Burton, D. R., McKeating, J. A., and Rice, C. M. (2005) *Science* **309,** 623–626
29. Reed, L. J., and Muench, H. (1938) *Am. J. Hyg.* **27,** 493–497
30. Albert, S., Will, E., and Gallwitz, D. (1999) *EMBO J.* **18,** 5216–5225
31. Du, L.-L., Collins, R. N., and Novick, P. J. (1998) *J. Biol. Chem.* **273,** 3253–3256
32. Hirokawa, T., Boon-Chieng, S., and Mitaku, S. (1998) *Bioinformatics* (*Oxf.*) **14,** 378–379
33. Wilson, B. S., Nuoffer, C., Meinkoth, J. L., McCaffery, M., Feramisco, J. R., Balch, W. E., and Farquhar, M. G. (1994) *J. Cell Biol.* **125,** 557–571
34. Monetta, P., Slavin, I., Romero, N., and Alvarez, C. (2007) *Mol. Biol. Cell* **18,** 2400–2410
35. Nuoffer, C., Davidson, H. W., Matteson, J., Meinkoth, J., and Balch, W. E. (1994) *J. Cell Biol.* **125,** 225–237
36. Allan, B. B., Moyer, B. D., and Balch, W. E. (2000) *Science* **289,** 444–448
37. Alvarez, C., Garcia-Mata, R., Brandon, E., and Sztul, E. (2003) *Mol. Biol. Cell* **14,** 2116–2127
38. Haas, A. K., Yoshimura, S.-i., Stephens, D. J., Preisinger, C., Fuchs, E., and Barr, F. A. (2007) *J. Cell Sci.* **120,** 2997–3010
39. Tisdale, E. J., Bourne, J. R., Khosravi-Far, R., Der, C. J., and Balch, W. E. (1992) *J. Cell Biol.* **119,** 749–761
40. Plutner, H., Cox, A. D., Pind, S., Khosravi-Far, R., Bourne, J. R., Schwaninger, R., Der, C. J., and Balch, W. E. (1991) *J. Cell Biol.* **115,** 31–43
41. Su, A. I., Cooke, M. P., Ching, K. A., Hakak, Y., Walker, J. R., Wiltshire, T., Orth, A. P., Vega, R. G., Sapinoso, L. M., Moqrich, A., Patapoutian, A.,

Hampton, G. M., Schultz, P. G., and Hogenesch, J. B. (2002) *Proc. Natl. Acad. Sci. U. S. A.* **99,** 4465–4470
42. Pfeffer, S., and Aivazian, D. (2004) *Nat. Rev. Mol. Cell Biol.* **5,** 886–896
43. Lanzetti, L., Rybin, V., Malabarba, M. G., Christoforidis, S., Scita, G., Zerial, M., and Di Fiore, P. P. (2000) *Nature* **408,** 374–377
44. Pei, L., Peng, Y., Yang, Y., Ling, X. B., van Eyndhoven, W. G., Nguyen, K. C., Rubin, M., Hoey, T., Powers, S., and Li, J. (2002) *Cancer Res.* **62,** 5420–5424
45. Haas, A. K., Fuchs, E., Kopajtich, R., and Barr, F. A. (2005) *Nat. Cell Biol.* **7,** 887–893
46. Miinea, C. P., Sano, H., Kane, S., Sano, E., Fukuda, M., Peränen, J., Lane, W. S., and Lienhard, G. E. (2005) *Biochem. J.* **391,** 87–93
47. Cuif, M. H., Possmayer, F., Zander, H., Bordes, N., Jollivet, F., Couedel-Courteille, A., Janoueix-Lerosey, I., Langsley, G., Bornens, M., and Goud, B. (1999) *EMBO J.* **18,** 1772–1782
48. Fuchs, E., Haas, A. K., Spooner, R. A., Yoshimura, S.-i., Lord, J. M., and Barr, F. A. (2007) *J. Cell Biol.* **177,** 1133–1143
49. Dabbeekeh, J. T., Faitar, S. L., Dufresne, C. P., and Cowell, J. K. (2007) *Oncogene* **26,** 2804–2808
50. Itoh, T., and Fukuda, M. (2006) *J. Biol. Chem.* **281,** 31823–31831
51. Zhang, X.-M., Walsh, B., Mitchell, C. A., and Rowe, T. (2005) *Biochem. Biophys. Res. Commun.* **335,** 154–161
52. Fukui, K., Sasaki, T., Imazumi, K., Matsuura, Y., Nakanishi, H., and Takai, Y. (1997) *J. Biol. Chem.* **272,** 4655–4658
53. De Antoni, A., Schmitzova, J., Trepte, H.-H., Gallwitz, D., and Albert, S. (2002) *J. Biol. Chem.* **277,** 41023–41031
54. Du, L.-L., and Novick, P. (2001) *Mol. Biol. Cell* **12,** 1215–1226
55. Machner, M. P., and Isberg, R. R. (2006) *Dev. Cell* **11,** 47–56
56. Murata, T., Delprato, A., Ingmundson, A., Toomre, D. K., Lambright, D. G., and Roy, C. R. (2006) *Nat. Cell Biol.* **8,** 971–977

TBC1D20 Is a Rab1 GTPase-activating Protein That Mediates Hepatitis C Virus Replication

Ella H. Sklan, Ramon L. Serrano, Shirit Einav, Suzanne R. Pfeffer, David G. Lambright and Jeffrey S. Glenn

J. Biol. Chem. 2007, 282:36354-36361.
doi: 10.1074/jbc.M705221200 originally published online September 27, 2007
